Article

Improved Low-Cost Home Energy Management Considering User Preferences with Photovoltaic and Energy-Storage Systems

Nedim Tutkun [1], Luigi Scarcello [2] and Carlo Mastroianni [2],*

[1] Department of Electrical & Electronics Engineering, İstanbul Ticaret University, 34840 İstanbul, Turkey; ntutkun@ticaret.edu.tr

[2] ICAR-CNR, Via P. Bucci, 8/9 C, 87036 Rende, Italy

* Correspondence: carlo.mastroianni@icar.cnr.it

Abstract: With smart appliances, it has been possible to achieve low-cost electricity bills in smart-grid-tied homes including photovoltaic panels and an energy-storage system. Apparently, many factors are important in achieving this and the minimization problem formulated requires a solution depending on a certain number of constraints. It should also be emphasized that electricity tariffs and the appliance operation type and range play a major role in this cost reduction, in particular, with dynamic electricity pricing usually available in a smart-grid environment. A limited number of metaheuristic methods are used to solve such a minimization problem, in which the start time of a controllable smart home appliance is the variable. However, the datasets used in many studies are different from each other and it is mostly unclear which of the proposed methods is better in this regard. In this study, we aim to minimize the daily energy consumption cost in a typical smart home with an energy-storage system integrated into a photovoltaic system under dynamic electricity pricing. While minimizing the daily energy consumption cost only, the user's discomfort and the peak-to-average ratio inevitably tend to increase, as expected. Therefore, a balance can be established among the objectives using multi-objective optimization. Solving this problem helps comparatively reduce the daily energy consumption cost, the peak-to-average ratio and the user's discomfort. The results are meaningful and encouraging for the optimization problem under consideration.

Keywords: home energy management; shuffled frog-leaping algorithm; multi-objective optimization; home appliance scheduling; electricity bill reduction

1. Introduction

Today it has become possible to achieve a significant reduction in the DC of electricity bills with DEP used in smart-grid-connected homes. Since it is a question of minimizing the DC of electricity bills, an MOO problem must be solved for optimal start-time values. Such optimization problems usually include three objectives, such as the DC, the PAR, and the UD. Supposing that the solution to the problem is simply to reduce the DC and ignore other objectives, namely, a single-objective optimization problem, is a low-cost solution to decrease the cost of the electricity bill and is called economy-mode operation. However, in such a solution, the operation lengths and intervals of smart HAs must be well-adjusted; otherwise, the power demand may reach the peak during the day when the DEP is the lowest, which may cause short-term damage until the insured protection is realized in the electrical installation of the residence. It is apparent that this would result in unexpected losses in local distribution lines when occurring in a large number of residences. In this regard, for an economic mode it is first necessary to determine the operation length and interval of each smart HA appropriately. Moreover, integrating a PV system and an ESS to the existing system in order to reduce the power demand from the grid offers both an economic and technical solution to the problem despite the investment and maintenance costs. Power scheduling can be performed by including the objectives of the PAR and

the UD; then, the single-objective optimization problem turns into a MOO problem. In this optimization problem, the weight coefficients are employed to construct the fitness function covering the three objectives. The weight coefficients in question are selected at appropriate values, mostly by trial and error, in accordance with the problem type and this is called intelligent mode of operation. The state of the art that forms the basis of this investigation is reviewed and given below.

1.1. State of the Art

Bouakkaz et al. proposed an approach to reduce the daily energy cost of smart household appliances using a PV array and an ESS in a grid-connected home as well as battery-loss consideration [1]. In this study, the day-ahead SR and the DEP data were used to schedule the operation of each appliance. The PSO algorithm was employed to solve the optimization problem and the DC was the only objective in the optimization problem.

Mohammad et al. considered a, HEMS with a PV system, an ESS and an EV battery storage to minimize the DC and the PAR by optimally scheduling the operations of the HAs [2]. This bi-objective optimization problem was solved for the start times of SHAs using the GWO algorithm. In this study, when the DEP was low, the HAs were supplied from the grid and the ESS was also charged from the grid if not fully charged or vice versa. In the case of surplus energy, it was used to charge the ESS and the rest was delivered to the grid when available.

Ahmad et al. designed an HEMS including a PV system and an ESS and aimed to lower the PAR and the DC using the GA, the binary PSO, the WDO, the BFO and hybrid GA-PSO algorithms [3]. In the optimization process, the day-ahead DEP, temperature and day-ahead SR were taken from the utility and the user's comfort objective was not considered. Dinh et al. proposed another study for an HEMS in which the ESS was integrated to the PV system to achieve possible savings in electricity bills in grid-connected homes [4]. The optimal starting times of smart HAs were found based on the day-ahead DEP and SR values taken from the local utility. This scheme aimed to store the energy for later use and sell it to the utility when the DEP is high, thereby reducing the overall DC. In this study, only the PAR and the DC were taken into account and in the proposed HEMS architecture, the BPSO algorithm was employed due to its suitability for on-and-off operation of smart HAs. The main disadvantage of the proposed system is that the excess energy is sold directly from the battery to the utility, thus reducing the overall system efficiency.

In another similar study by Merdanoglu et al., the MILP technique was used to optimally schedule the operation of smart HAs in the proposed HEMS supplied from the grid, wind turbines, a PV array and the ESS [5]. Furthermore, the real-time sold and purchased electricity prices, estimation of wind speed and SR values and consumer behaviour for planned and unplanned load cases were taken into account during the optimization process, but the PAR and the household's comfort were not considered. Wang et al. carried out another study about the low-cost operation of the SAs in a designed grid-tied HEMS including a PV array and ESS using the BA [6]. However, in this study, the PAR was not considered, the number of HAs was few and the operation types of them and the DEP were not taken into account.

Amer et al. proposed another HEMS that included EVs, all types of NSHAs and SHAs, a PV system and an ESS using the interior-point method [7]. In this study, users can only perform demand-response actions and the scheduling of the loads is optimized based on the pricing schemes. The user's comfort, cost reduction and the distribution transformer's loss of life were the objectives of the problem. Dinh et al. suggested a new HEMS, unlike the conventional HEMS, which usually controls or schedules appliances to monitor energy usage, minimize energy cost and maximize user comfort [8]. In this study, the proposed hour-ahead demand-response strategy first learns the appliance-usage behaviour of the residents; with this knowledge it controls the ESS and the PV system to lower the daily energy cost. The training datasets are created from the optimal outputs of the MILP solver using historical data. Ma et al. presented a self-regulating HEMS to

minimize the daily energy costs by optimally scheduling HAs, a PV system, and the ESS, as well as the charging and discharging of EVs [9]. In this study, power consumption and generation were not only optimally scheduled in the proposed HEMS but also the timely purchase of electricity from the grid and the PV system were optimally scheduled.

Song et al. studied an intelligent HEMS with PVs and an ESS to maximize the economic benefits and consumers' comfort based on a tri-objective model concerning different weight coefficients to reach a balance among the running costs, the peak–valley balance index and the satisfaction index [10]. Koltsaklis et al. investigated a smart HEMS that includes flexible appliances, a PV array, wind turbines, EVs, an ESS and the DEP to minimize energy costs using ML for highly accurate demand forecasting [11]. Chakir et al. proposed a management system equipped with a grid-tied hybrid system composed of a PV array, a wind turbine and an ESS using LP with constraints in order to reduce the energy cost due to the smart HAs' power consumption [12]. Lissa et al. used DRLA for indoor and domestic hot-water temperature control, aiming to reduce the energy consumption by optimizing the usage of PV energy production [13]. Furthermore, a methodology for a new dynamic indoor temperature set point definition was presented, thus allowing greater flexibility and savings to the increase user's comfort and decrease the DC for smart HEMS based on a feasible solution. Huang et al. proposed an hour-ahead demand-response algorithm for an HEMS using an artificial neural network approach that uses stable cost predictions as a method for dealing with upcoming price uncertainties [14]. In this study, for making optimum and decentralized decisions for various household devices, multi-agent reinforcement learning was used along with predicted upcoming costs. Parandeh et al. proposed OCDM for day-ahead dynamic pricing of grid-connected residential renewable energy resources under different metering mechanisms: feed-in-tariffs, net metering and net purchase and sale in conjunction with carbon emission taxes [15]. According to the stochastic nature of consumers' load and PV-system products, uncertainties were considered in a two-stage decision-making process. In addition, it is seen in the literature that the SFLA technique has been modified with well-known AI methods and used to solve current energy-management problems in hybrid electric vehicles and water-resource systems. Debata et al. proposed an approach to improve energy management in hybrid electric vehicles [16]. In this study, energy management was formulated as an optimization problem and the problem was solved using the SFLA modified by the ANN. The results indicated that the proposed approach worked well and yielded meaningful and encouraging outcomes compared to those obtained from similar works. In another similar study by Fang et al., a multi-objective DE-CSFLA was proposed for water-resource system optimization [17]. The obtained results showed that the proposed method exhibited better performance than those used for similar problems.

Finally, examining the above-mentioned studies from various aspects, very few studies have addressed a MOO problem covering the three objectives from various aspects. The most recent studies mentioned above are briefly summarized in Table 1, which specifies whether such studies take into consideration the three objectives (the DC, the PAR and the UD), and whether the related systems exploit RES and the ESS. In the Table, Y and N stand for "yes" and "no", respectively.

1.2. The Original Contribution

In the problem at hand, the operation of a controllable smart HA can be represented by 1 and not by 0. Thus, the operation of any smart HA in an operation range can be expressed by a binary string, and random possible binary solutions can be generated for each electrical household appliance. It can be said that the ability to solve this non-convex complex optimization problem with the binary-coded GA is better than other methods due to its advanced operators. The main reason for this is that there are two advanced genetic operators in the GA, such as crossover and mutation. With these operators, the possibility of producing different individuals in the population, especially by crossover, is higher than other methods, so that the specific crossover operator can be developed for the

problem. With mutation, it is possible to overcome problems such as early convergence in the genetic process. Although the SFLA is similar to other metaheuristic methods, it converges to the global best individual in a short time by continuously improving the worst individual in the population. Thus, it presents an advantageous condition in finding the global optimal. A new crossover technique specifically developed and combining these prominent advantageous features of GA and the SFLA is called the GA-SFLA and it is presented as a new approach to solving the problem. It is seen that metaheuristic methods such as PSO, GWO and BFO give similar results to the results obtained from using SFLA or GA.

Table 1. The main and most recent studies.

Ref.	DC	PAR	UD	RES	ESS	Method
[1]	Y	N	N	Y	Y	PSO
[2]	Y	Y	N	Y	Y	GWO
[3]	Y	Y	N	Y	Y	BFO, WDO
[4]	Y	Y	N	Y	Y	BPSO
[5]	Y	N	N	Y	Y	MILP
[6]	Y	N	Y	Y	Y	BFO
[7]	Y	N	Y	Y	Y	IPM
[8]	Y	N	Y	Y	Y	MILP
[9]	Y	N	N	N	Y	AI
[10]	Y	Y	Y	Y	Y	MILP
[11]	Y	N	Y	Y	Y	ML
[12]	Y	N	Y	Y	Y	LP
[13]	Y	N	N	Y	N	DRLA
[14]	Y	N	N	Y	N	ANN
[15]	Y	N	N	Y	N	OCD
[16]	Y	N	N	Y	N	SFLA-ANN
[17]	Y	N	N	Y	N	DE-CSFLA

The rate of convergence and failure rate in the GA-SFLA vary according to the nature of the problem. Considering this problem, the convergence rate is less than 1 min in offline operation, depending on the required parameter values. It is known from the literature that the problem-solving capacity of the GA is higher than other metaheuristic methods. Here, we attempt to make it better with problem-specific improvements.

In this study, it is expected to minimize the daily energy-consumption cost in a typical smart home under dynamic electricity pricing with the ESS integrated into the PV system. While achieving this objective, the UD and the PAR values were maintained at the lowest possible values using multiple optimization. In the solution to this problem, the day-ahead DEP and SR values are obtained from the utility and the WDC at 23.00 every day. As a result of the non-convex multiple-optimization made with the data provided, the optimal operation scheduling data of that day are transferred to the EMC, which controls the smart Has' on/off. The operation start time of each controllable smart HA is considered as an optimization or decision variable. In the relevant literature, it is seen that a limited number of population-based metaheuristic methods inspired by natural life are used in the solution of such problems. In each of these methods, an iterative improvement is made within the determined rules from the possible solutions. Among these, the SFLA is subject to continuous improvement of the worst individual and a genetic algorithm produces more diversity with crossover and mutation operations in the possible solutions. The novelty and contribution of this study is that these two features of the methods are combined and a problem-specific crossover is developed to solve the multi-objective optimization problem under consideration. The results obtained are compared with the results of the previous study [8], and it is shown that the proposed approach performed better results.

2. Materials and Methods

In this section, the HEMS architecture, problem definition and proposed approach are particularly described from many aspects.

2.1. HEMS Architecture

In this study, three types of HEMS called HEMS1, HEMS2 and HEMS3 were used. HEMS1, as shown in Figure 1, is connected to the smart grid and consists of the metering infrastructure, a smart energy meter, a home gateway, EMC, smart SHAs and NSHAs. HEMS2 is built by additionally integrating a PV system generating a maximum power of 1.8 kW and a 10 kWh ESS that can charge and discharge 0.95 kW per hour to HEMS1. HEMS3 is a special case of HEMS2 that is formed by increasing the capacity of the PV system in HEMS2 by 50%. The DEP signal transmitted to HEMS1, HEMS2 and HEMS3 contains the hourly day-ahead DEP sent to the user through the utility at 23:00. The optimal start times of the smart HAs are found by performing single-objective optimization and MOO to produce the lowest cost for the DEP provided. The EMC makes the smart HAs operate at the optimal start times for a day and a similar procedure is repeated the next day.
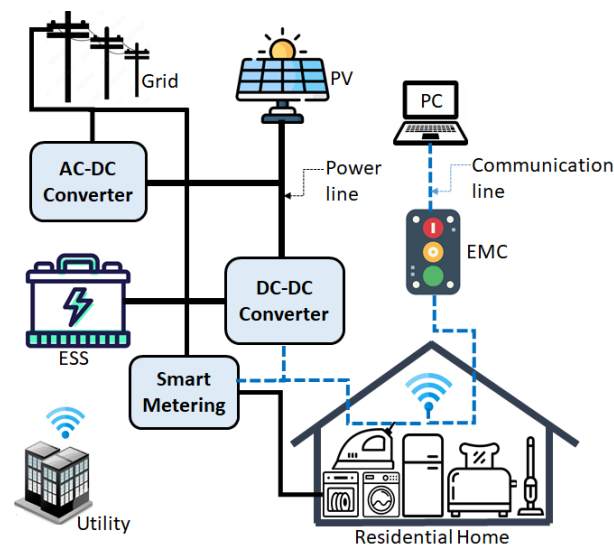

Figure 1. The basic architecture of the HEMS with a wireless home area network.

If the user desires to optimally schedule the smart HAs, he/she acquires the optimal scheduling results by running the MATLAB R2022b after receiving the DEP and SR data for the next day from the smart-grid utility and the WDC. These results are then transmitted to the EMC and presented for the user's approval on the screen. If the user desires to comply with this schedule for the next day, he/she performs the optimal scheduling by giving the necessary approval on the EMC screen shown in Figure 1.

If the user does not approve, he/she continues to use the electrical HAs manually. Optimal scheduling is carried out daily, and each household appliance starts working at the starting time specified in the schedule and works for the operation length specified. The block diagram of the operation of the whole system is shown in Figure 2.

2.2. Defition of SSAs and NSSAs

The SHAs and NSSAs are shown in Table 2. The SHAs have a certain operation range and uninterruptible operation length, and the power absorbed by each appliance is constant during its operation. The DC, the PAR and the UD are optimized by shifting the start times of smart SHAs back or forth within the range they operate. The appliances used in the second category have a certain operating range and uninterruptible operation length, and the power absorbed by each appliance is unchanged during its operation. The start times

of the NSSAs cannot be shifted back or forward in the range they operate; that is, the start times are always the same for next-day operation.
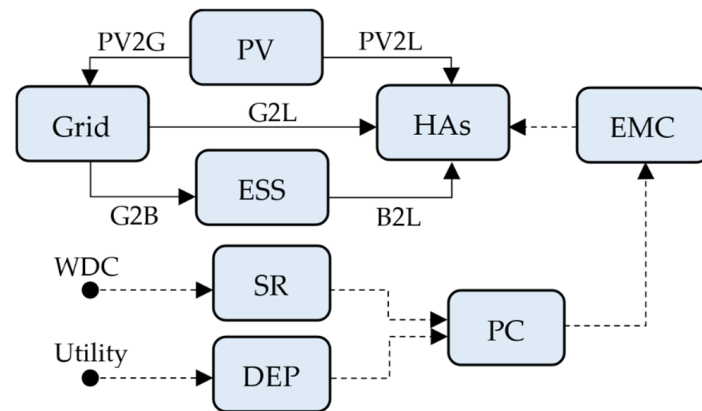

Figure 2. The block diagram of the whole-system operation.

Table 2. The smart SHAs and NSSAs used in this study [8].

Type	Appliance	P	L	SS	ES	BSS
SHA	TO	0.8	1	2	10	8
	IR	1.1	1	2	13	7
	VC	0.7	1	9	20	11
	MW	0.9	1	9	19	12
	EK	1	1	5	12	7
	AC	1.3	10	6	24	10
	WM	1	2	8	21	10
	CD	1.8	1	10	23	12
	CO	0.6	2	16	21	18
	DW	1.4	2	17	24	20
	SH	2.5	1	18	24	21
	HD	1	1	21	24	22
NSHA	PC	0.2	14	9	22	9
	SC	0.1	24	1	24	1
	RG	0.9	21	3	17	3
	TV	0.2	6	17	10	10
	LI	0.1	7	18	10	10

2.3. PV System

The PV system consists of 6 monocrystalline 300 W panels installed on the roof of the home. This system produces a maximum of 1.8 kW of power, as shown in Figure 3, during the day and includes an MPPT to ensure the maximum power generation under changing environmental conditions. According to Figure 3, the generated power is the highest between 12.00 and 16.00 h, as expected, while it becomes zero between 0.00 and 7.00 and between 21.00 and 24.00 h. The main advantage of using PV in such systems is that the PV system produces the most power during the time when the DEP is mostly highest. Only one power curve was used in this study in order to make a consistent comparison

of the proposed approach with a previous study [8]. The power produced by the system depends on the SR and the energy produced at time slot t is calculated by:

$$E_{PV}^{(t)} = G^{(t)} S \Delta t \eta_{PV} \tag{1}$$

where $G^{(t)}$, S, Δt and η_{PV} are the amount of SR coming to the surface, surface area, time period in hours and PV efficiency in time slot t, respectively, and the constraint $0 \leq E_{PV}^{(t)} \leq 1.8$ kWh must be satisfied.
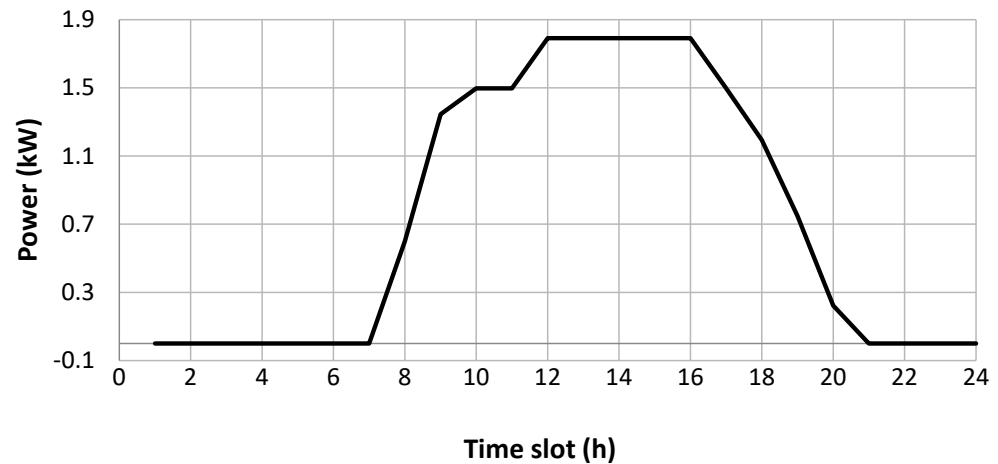

Figure 3. PV power variation with time slot [8].

2.4. Defition of ESS

The total capacity of the ESS consisting of a group of Li-Fe-PO4 batteries is considered to be 10 kWh and the charging and discharging power and efficiency are 1 kW and 0.95, respectively. The amount of energy stored at time interval t can be found by:

$$E_{ESS}^{(t+1)} = E_{ESS}^{(t)} + u^{(t)} E_{CD}^{(t)} \eta_C \tag{2}$$

where $E_{CD}^{(t)}$ and η_C are the amount of energy charged or discharged at time interval t and the charge or discharge efficiency, respectively. The constraints $0 \leq E_{CD}^{(t)} \leq 1$ kWh and 0.5 kWh $\leq E_{ESS}^{(t)} \leq 10$ kWh must be satisfied during charging and discharging operations. u^t is the operation mode of the ESS at time interval t and it is 1 in the charging case, -1 in the discharged case and 0 when there is no charging or discharging action.

2.5. Problem Definition

In this study, the DC in a typical smart home equipped with an ESS integrated into the PV system under DEP is minimized. The UD and the PAR values were maintained at the lowest values while achieving this goal during a multi-optimization process. In the solution of this problem, the DEP and SR values are obtained from the smart-grid utility and from the local meteorological station at the end of the day. As a result of the non-convex MOO made with these data provided, the optimum operation-scheduling data of that day are transferred to the EMC, which controls the switching on and off of smart HAs. The start-up time of each controllable smart home device is considered to be a decision variable.

For better understanding of optimal scheduling, a day is divided into 24 evenly spaced time slots; hence, the shortest time interval is an hour. In other words, each SHA or NSHA must operate for at least an hour. Let T be a set of time slots that can be defined by:

$$T = \{1, 2, 3, \dots, 24\}, \forall t \in T \tag{3}$$

It is assumed that the operation time of each SA is a minimum integer multiple of an hour. There is a defined range in which each SSA or NSSA is operated in daily use and the main objective here is to find the best start times to make the DC lowest, depending on the DEP. Let A be a set of smart SHA that can be defined as:

$$A = \{a_1, a_2, a_3, \ldots, a_i, \ldots, a_n\} \tag{4}$$

where a_i is the ith uninterruptible SHA in the set of A.

The average power consumption vector for a_i can be expressed as:

$$P_{a_i} = \left[p_{a_i}^{(1)}, p_{a_i}^{(2)}, \ldots, p_{a_i}^{(t)}, \ldots, p_{a_i}^{(24)} \right] \tag{5}$$

where $p_{a_i}^{(t)}$ is the average power delivered to a_i at the time interval t.

A more detailed definition is made as follows:

Let $\alpha_{a_i}, \beta_{a_i} \in T$ be the first and last values of the operation interval, respectively, and $\alpha_{a_i} < \beta_{a_i}$. In addition, let l_{a_i} be the operation length for a_i and $l_{a_i} \leq \beta_{a_i} - \alpha_{a_i}$.

Hence, let $\gamma_{a_i} \in [\alpha_{a_i}, \beta_{a_i} - l_{a_i} + 1]$ be the possible start times of uninterruptible a_i. The start time is considered to be an optimization variable of each smart HA. Thus, from the above definitions, the power demand function for a_i can be expressed as:

$$p_{a_i}^{(t)} = \begin{cases} P_{a_i}, & \gamma_{a_i} \leq t \leq \gamma_{a_i} + l_{a_i} - 1 \\ 0, & \text{otherwise} \end{cases} \tag{6}$$

For instance, a_i's operation range is 1 to 8 slots, and its operation length is 1 slot. Accordingly, the start time of a_i is any integer value between slots 1 and 8. This value may be 1 or 8. Let us assume a_i's operation length is 2 slots. In this case, a_i's start time is any integer value from slots 1 to 7. The value "-1" is used to determine the exact start time of a_i as a slot.

Hence, the total average power consumption for SHAs or NSHAs can be calculated by:

$$P_{top} = \sum_{t=1}^{24} \left(\left(\sum_{i=1}^{m} p_{a_i}^{(t)} \right) + \left(\sum_{j=1}^{n} p_{b_j}^{(t)} \right) \right) \tag{7}$$

where m is the total number of SHAs, n is the total number of NSHAs, and $p_{a_i}^{(t)}$ and $p_{b_j}^{(t)}$ are the average power consumption for the SHA and the NSHA, respectively, at the slot t.

2.6. Optimization Process

The implementation of the optimization algorithm on the problem under consideration is explained in the sections below.

2.6.1. Single-Objective Optimization

In general, the total DC can be calculated by:

$$C_T = \frac{\sum_{t=1}^{24} \left(\left(E_{G2L}^{(t)} + E_{G2B}^{(t)} \right) pr_p^{(t)} - \left(E_{B2G}^{(t)} + E_{PV2G}^{(t)} \right) pr_s^{(t)} \right)}{C_{T_{max}}} \tag{8}$$

where $pr_p^{(t)}$ and $pr_s^{(t)}$ are the energy price purchased from the grid and the energy price sold to the grid for the constraint $pr_p^{(t)} = \sigma pr_s^{(t)}$ and σ is one for simplicity. $E_{G2L}^{(t)}$ is the energy delivered from the grid to the load, $E_{G2B}^{(t)}$ is the energy delivered from the grid to the ESS, $E_{B2G}^{(t)}$ is the energy delivered from the ESS to the grid and $E_{PV2G}^{(t)}$ is the energy delivered from the PV to the grid. Moreover, $C_{T_{max}}$ is the maximum possible total DC, that is, 837.4¢. Note that if the ESS and PV system are unavailable, $E_{G2B}^{(t)} = 0$, $E_{B2G}^{(t)} = 0$, $E_{PV2G}^{(t)} = 0$ and $\forall t \in T$ in Equation (8).

Equation (8) expresses the total cost proportionally and is also expressed as an objective function for the single optimization process. The value of 837.4¢ is the maximum daily total cost possible corresponding to the highest value of 27.5¢ among the current DEP. Very short-term changes in electricity prices such as 1 or 5 min, hourly or less-optimal scheduling and performance of the battery depending on the environmental effects, temperature changes, surface contamination and shading of the PV require a complex calculation in finding the DC and make the solution of the problem difficult.

Since the aim is to minimize the DC, Equation (8) is rearranged to construct the normalized fitness function of the DC expressed as:

$$f_{C_T} = \min(C_T) \tag{9}$$

To find the lowest cost for HEMS based on Equation (8) the deterministic minimization algorithms, namely Algorithms 1 and 2, are defined as follows:

Algorithm 1: Minimum cost for an SHA with 1-h length.

---

1. Define each SHA with 1-h length and other initial parameters
2. Create a 24 × 1 zeros matrix for each SHA
3. Generate an index in an operation range for each SHA
4. Find the index value corresponding to the lowest price in the operation range for each SHA and change the zero to one in that index value.
5. Calculate the power vector for each SHA by multiplying the resulting binary string with the rated average power.

Algorithm 2: Minimum cost for an SHA with more than 1-h length.

---

1. Define each SHA with more than 1-h length and other initial parameters.
2. Create a 24 × 1 zeros matrix for each SHA.
3. Calculate end slot index in a given range and generate indices in between start and end slots for each SHA.
4. Calculate the cost during the operation in the given range for each SHA in a loop.
5. Find the lowest cost in the resulting cost vector.

2.6.2. Multi-Objective Optimization

Since there are large differences between the objective function values for the DC, the PAR and the UD, each function value is normalized. In this respect, the DC is divided by the highest cost that occurs during the day to find the normalized DC. Similarly, the normalized UD is calculated by dividing the UD by the maximum waiting time. Hence, the normalized UD_{a_i} or the normalized waiting time for a_i is calculated by

$$UD_{a_i} = \frac{|XSS_{a_i} - BSS_{a_i}|}{(UD)_{max}} \tag{10}$$

where XSS_{a_i} and BSS_{a_i} are an arbitrary start slot and the best start slot for a_i, respectively. $(UD)_{max}$ is the maximum waiting time of 24 h. Moreover, in Equation (10), the constraints $\alpha_{a_i} \leq XSS_{a_i}, BSS_{a_i} \leq \beta_{a_i}$ must be satisfied in any case.

Hence, the normalized fitness function of the UD can be calculated by:

$$f_{UD} = \min\left(\sum_{i=1}^{m} (UD)_{a_i}\right) \tag{11}$$

In order to formulate the PAR objective function, the PAR can first be found by dividing the maximum power demand at time slot t by the average power demand for SHAs and it can be given by:

$$PAR = \frac{Max\left(\left(\sum_{i=1}^{m} p_{a_i}^{(t)}\right) + \left(\sum_{j=1}^{n} p_{b_j}^{(t)}\right)\right) / P_{ave}}{PAR_{max}} \tag{12}$$

where P_{ave} is the average power demand, PAR_{max} is the maximum PAR, that is, 11.7 kW, and $t \in T$.

Thus, the normalized fitness function of the PAR can be expressed as:

$$f_{PAR} = \min(PAR) \tag{13}$$

where the expression in the numerator represents the PAR, while the expression in the denominator shows the maximum PAR occurred during the day and always remains the same.

It is now possible to create a single fitness function with the weighting coefficients to be selected appropriately by using the objective functions mentioned above. Thus, the combined fitness function is expressed as:

$$f = \min\left(\omega_1 f_{C_T} + \omega_2 f_{UD} + \omega_3 f_{PAR}\right) \tag{14}$$

In the case of a single-cost optimization, $\omega_1 = 1$ and the other weight coefficients are zero. Based on an optimization to reduce the DC, the UD and the PAR, it must take values between 0 and 1 to satisfy the constraint $\omega_1 + \omega_2 + \omega_3 = 1$ (e.g., $\omega_1 = 0.8$, $\omega_2 = 0.1$ and $\omega_3 = 0.1$). The logic used in this selection is that we selected the weight coefficients the same as those in a previous study [8] for a fair comparison. The weighting coefficients varied from 0.1 to 0.5 to see their effect on the objective functions. For instance, as the weight coefficient decreases, the optimal value of the objective function in question increases, and in the opposite case, the optimal value decreases.

2.7. The Proposed Method

The application of the proposed method to the problem under consideration is explained in Sections 2.7.1 and 2.7.2.

2.7.1. The Modified SFLA Algorithm

The modified SFLA is a global-search-optimization technique based on the memetic evolution of a group of frogs aiming to explore the best location for food available. It contains a few search elements to exchange information among the frogs to improve the current solutions. The SFLA starts with a randomly generated population F with N virtual frogs and it can be defined by:

$$F = \{x_1, x_2, x_3, x_4, ..., x_{N-1}, x_N\} \tag{15}$$

The population is then partitioned into subpopulations or memeplexes with a certain number of frogs. The number of memeplexes usually depends on the population size and it should be at least a quarter of the population size. The position of each individual in a memeplex is subject to change during memetic evolution and there is a constant improvement by making the worst individual better than before. To briefly formulate the algorithm, let the population size and the number of memeplexes be u and v, respectively; hence, the dimension of search space can be defined by:

$$F = \begin{bmatrix} x_{11} & x_{12} & \ldots & x_{1j} & \ldots & x_{1v} \\ x_{21} & x_{22} & \ldots & x_{2j} & \ldots & x_{2v} \\ \vdots & \vdots & \vdots & \vdots & \vdots & \vdots \\ x_{i1} & x_{i2} & \ldots & x_{ij} & \ldots & x_{iv} \\ \vdots & \vdots & \vdots & \vdots & \vdots & \vdots \\ x_{u1} & x_{u2} & \ldots & x_{uj} & \ldots & x_{uv} \end{bmatrix} \tag{16}$$

Each memeplex or subpopulation has a worst and best individual defined as x_w and x_b, respectively, and the global best x_g is the most-fitted individual in the whole population. For the improvement of the worst individual, it is first performed by Equation (17a). If no improvement is achieved with this equation, Equation (17b) is used. If no improvement is achieved in both cases, it is taken as a random value in the search space determined by Equation (17c) for the relevant variable:

$$x_{jw}^{(k+1)} = x_{jw}^{(k)} + r\left(x_{jb}^{(k)} - x_{jw}^{(k)}\right) \tag{17a}$$

$$x_{jw}^{(k+1)} = x_{jw}^{(k)} + r\left(x_{g}^{(k)} - x_{jw}^{(k)}\right) \tag{17b}$$

$$x_{jw}^{(k+1)} = \left(b_n - a_n\right)r + a_n \tag{17c}$$

where $x_{jw}^{(k)}$ and $x_{jb}^{(k)}$ are the worst and best frogs, respectively, in the jth memeplex for the kth generation, a_n and b_n are the lower and upper bounds, respectively, for the relevant search space and r is a uniformly distributed random number between 0 and 1.

A simple improvement of the worst individual is shown in Figure 4. As seen from Figure 4, a frog in the worst position at point A aims to reach point D where the food is in the shortest way and of course in the shortest time in order to find food.
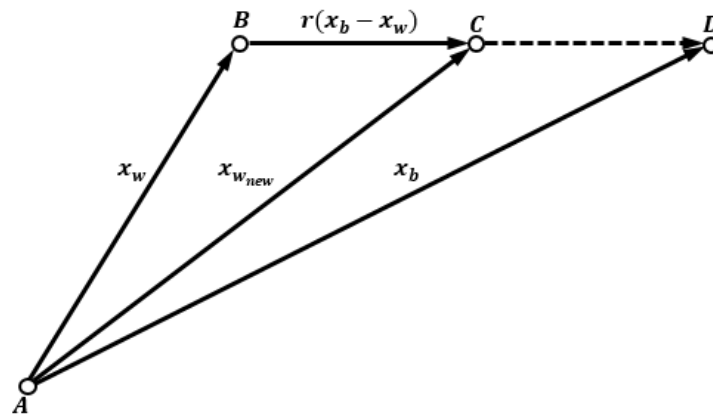

Figure 4. The original frog-leaping rule.

The frog in the worst position reaches point B first with the information obtained from its environment and reaches point C by making a random update using the location information of the best and worst frogs. It continues at point C with a similar update to the one it made at point B, and finally arrives at point D. Once the evolution process is completed in each subpopulation, the subpopulations are again structured into a single population and the fitness value is calculated for each individual of the population. The fitness values are then ordered from smallest to largest and the global best fitness is determined as the first individual. Next, the sorted individuals are reshuffled into each memeplex according to their fitness values, as previously explained.

Finally, the global optimum solution is found by continuing the optimization process until the maximum number of iterations is reached. In order to obtain different possible solutions, besides generating random numbers between 0 and 1, crossover and mutation operators are used. In the designed MATLAB R2022b the number of memeplexes is 32, the population size for each memeplex is 100, the maximum generation number is 100 for each memeplex and the total generation number is 100. The main flowchart of the SFLA and its local search algorithm are illustrated in Figures 5 and 6.
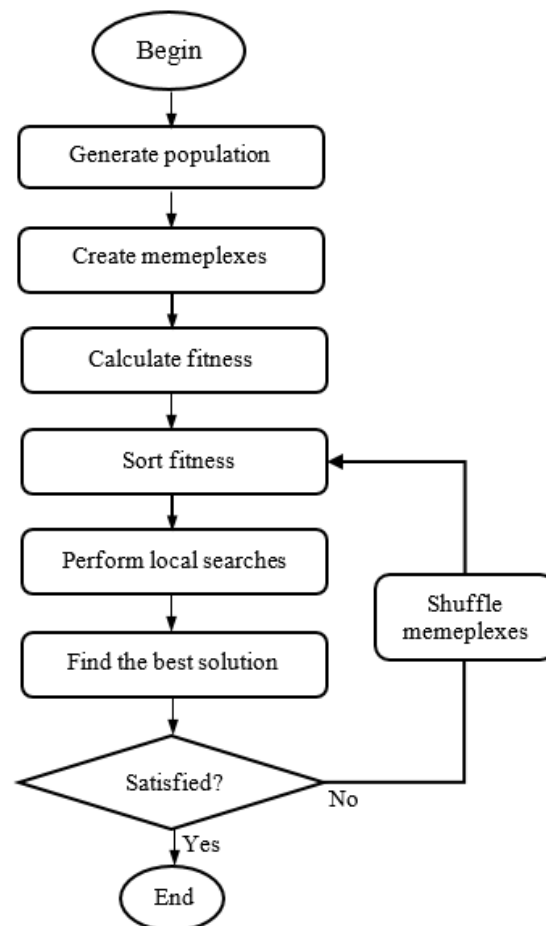
Figure 5. The flowchart of the SFLA.

2.7.2. The Developed Crossover Operation

In the local optimization process, a newly developed crossover algorithm is used to generate dissimilar individuals for the improvement of the worst individual. In this algorithm, the start slots of the SHAs are randomly shifted to the right or left according to their suitability. With the distinct individuals obtained by this approach, the improvement of the worst individual in the subpopulation is mostly made. The crossover operation is given in Algorithm 3.

As a result, the proposed method is used in the context of different scenarios to solve the multi-objective optimization problem using the modified SFLA. The obtained results are given in Section 3.
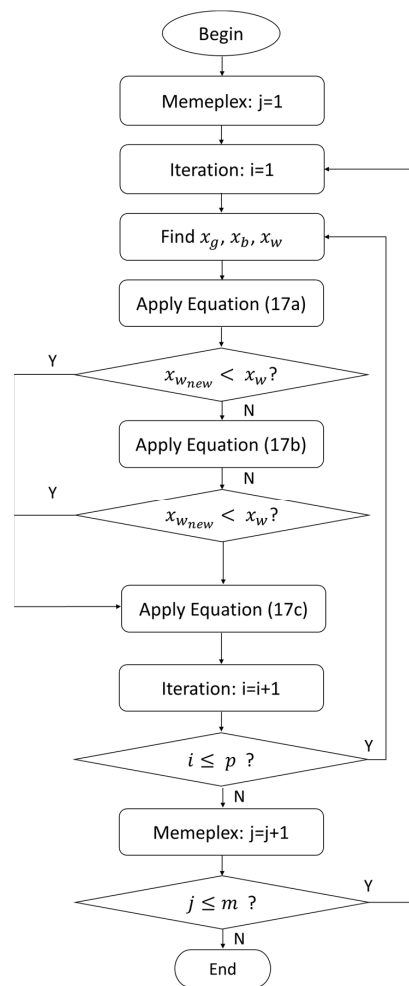
Figure 6. Flowchart of the local search.

Algorithm 3: Crossover operation for SFLA.

---

1. Enter the string and the first and last indices of the operation range
2. Create substring in operation range
3. Determine the number of elements of the substring
4. If the first element of the substring is equal to 1,
4.1 Find the indices corresponding to the ones in the substring
4.2 Create a new substring of zeros in the same size of the old substring
4.3 Increment the indices by 1 and set the values corresponding to these indices to one
5. If the last element of the substring is equal to one,
5.1 Find the indices corresponding to the ones in the substring
5.2 Create a new substring of zeros in the same size of the old substring
5.3 Decrement the indices by one and set the values corresponding to these indices to one
6. If (3) and (4) are not the case,
6.1 Generate a random number between 0 and 1.
6.2 If the number is greater than and equal to 0.5, find the indices of substring corresponding to one
6.3 Create a new substring of zeros in the same size of the old substring
6.4 Increment the indices by one and set the values corresponding to these indices to one
6.5 If the number is less than 0.5, find the indices of substring corresponding to one
6.6 Create a new substring of zeros in the same size of the old substring
6.7 Decrement the indices by one and set the values corresponding to these indices to one
7. Create a new string of zeros in the same size of the old string
8. Copy the substring at hand to this string.

---

3. Results and Discussion

The simulation process based on the designed software was carried out with a laptop computer with an Intel(R) Core(TM) i5-CPU@1.60 GHz, 16 GB RAM and Windows 10 Pro (64-bit). The computational time to obtain the simulation results for single-objective and multi-objective optimization was less than a minute and this seems to be reasonable for this kind of application. In the single optimization, the start times of the SHAs are optimized with a deterministic optimization algorithm within the operation intervals to give the lowest DC. Since this optimization is based solely on the cost, the cost naturally decreases while the PAR and the UD values increase relatively. In the second optimization, the cost was optimized by converting the DC, the PAR and the UD objectives to a single-objective function with their selected weight coefficients. As expected in this optimization, the weight coefficients play an important role in optimizing the objectives. The simulation results were obtained for the HEMS1 and HEMS2 cases under certain constraints and conditions. The results were compared to the results of the non-HEMS condition to see the improvement in both HEMS conditions as well as the results of previous work [8].

The optimization process was carried out based on the DEP shown in Figure 7. As seen in Figure 7, the DEP reaches its highest value of 27.5¢ between 09.00 and 10.00 h and the lowest value of 8¢ between 19.00 and 20.00 h.
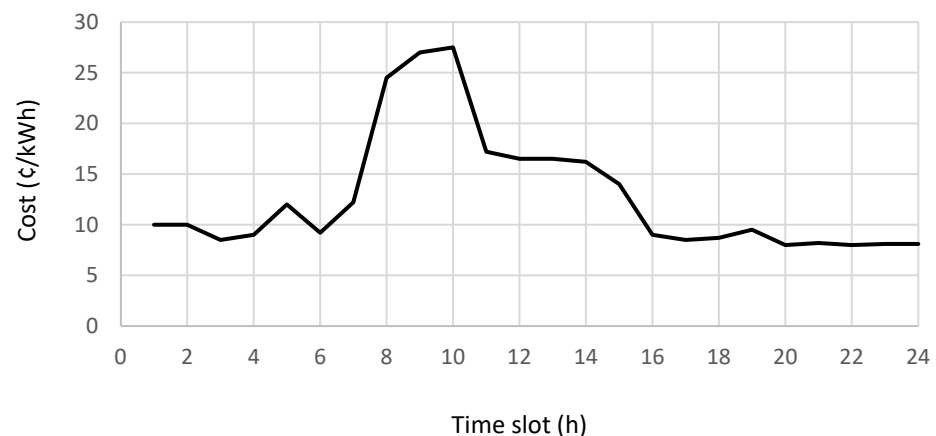

Figure 7. Day-ahead DEP provided by the utility.

In order to further reduce the DC in the HEMS1, the HEMS2 was created by integrating the PV system and the ESS with the grid-connected HEMS1. However, although this integration brings investment and maintenance costs to the overall cost, it provides a significant advantage in reducing the DC, the PAR and the UD and it has been possible to quantify the confirmation on the same SHAs used in a similar study [8]. It should be emphasized here that if the optimization problem under consideration was not solved by the proposed method or similar methods, the best possible approach would be to increase either the ESS capacity or the PV-system installed capacity to obtain the same DC, PAR and UD values.

3.1. Results of Single-Objective Optimization

In this optimization process, the lowest cost that can occur in HEMS1 and HEMS2 under the current conditions was found using the deterministic optimization algorithm. In this algorithm, the start time that gives the lowest DC in its operation range was determined for each SHA. Accordingly, the cost of SHAs for HEMS1 and HEMS2 was 247¢ and 197¢, respectively, while the total DC was 582.9¢ and 177.5¢, respectively. The starting slot and cost for each SHA are given in Table 3 for both non-HEMS and HEMS study cases. As can be seen from Table 3, an improvement of 32.2% and 44.4% was achieved in the DC of HEMS1 and HEMS2, respectively. In both cases, the major improvement was with the cost savings in the toaster.

Table 3. Comparison of the DC for various HEMS.

SHA	Non-HEMS	HEMS1	HEMS2	BSS	LCSS
TO	19.6	6.8	5.5	8	3
IR	13.4	9.4	7.5	7	3
VC	12.0	5.6	4.8	11	20
MW	14.9	7.7	6.1	12	17
KE	12.2	9.2	6.8	7	6
AC	186.7	117.1	89	10	15
WM	44.7	16.2	14	10	20
CD	29.7	14.4	12	12	22
CO	10.9	9.7	8.2	18	20
DW	22.7	22.5	19	20	22
SH	20.5	20.0	17	21	20
HD	8.0	8.2	6.8	22	21

This implies that in order to save money, the toaster must operate 5 h before its best start time, that is, at 02:00 and the washing machine should operate with a delay of 10 h. The total UD is higher than that in the best-time operation of the SHAs. Furthermore, the PAR is found to be 2.37 and 3.33, respectively, and this means that the power demand in a one-hour period reaches 2.37 or 3.33 times the average power value for the designed HEMS1 and HEMS2. As shown in Table 3, the daily consumption cost of each SHA is lower in HEMS2 compared to that in HEMS1.

This is because some of the energy needs of SHAs and NSHAs are met from the PV and ESS rather than from the grid, as shown in Figure 8. The total cost was calculated as 731.1¢, 582.9¢ and 374.1¢, respectively, for the non-HEMS, HEMS1 and HEMS2 cases. As seen from Table 3, the cost was found to be lowest for SSAs in and below this value; it is not possible to reach a lower cost value. As can be seen from Figure 8, in the HEMS2, the ESS is charged and discharged with a value in the range of 0–0.95 kW during a slot when the DEP is the lowest and the highest, respectively, and at the end of the day significant savings are achieved. However, only the DC objective is focused on here, and the PAR and the UD objectives are not considered. In other words, in order to minimize the PAR and the UD at the same time, it is necessary to approximate the start times to BSS values. Since multiple optimizations are required for this, multiple optimizations were performed for both HEMS1 and HEMS2 under the current conditions and constraints.
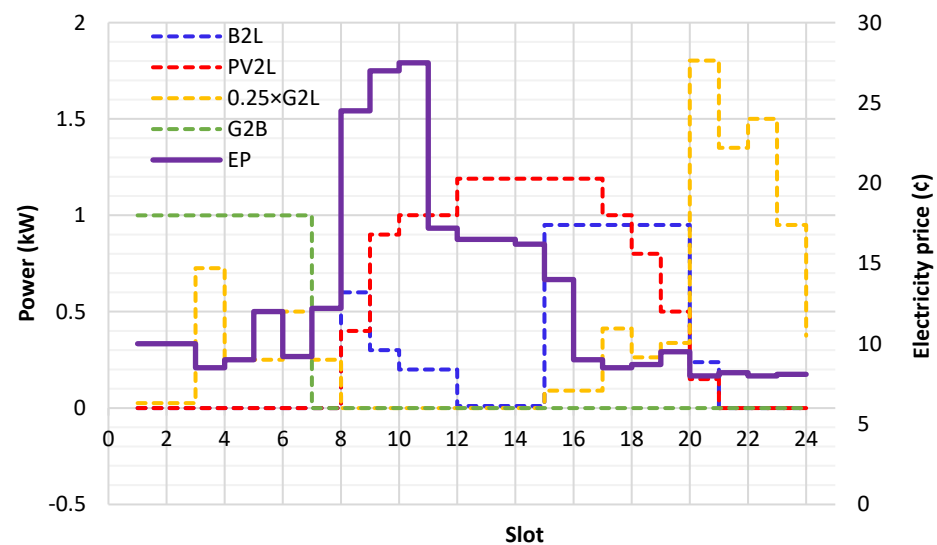
Figure 8. Power variation with time slot in the SOO.

3.2. Results of Multi-Objective Optimization

In this optimization process, the cost, the PAR and the UD objectives for HEMS1 and HEMS2 were optimized using the SFLA method under the current conditions and constraints. With the weight coefficients, it is possible to reduce the three objective functions to a single-objective function. The optimization involves the minimization of each objective, and the value of the weight coefficient has more influence on this process. The optimal cost for HEMS1 was found by first taking the weight coefficients $w_1 = 0.8$, $w_2 = 0.1$ and $w_3 = 0.1$; second, $w_1 = 0.7$, $w_2 = 0.1$ and $w_3 = 0.2$; and finally, $w_1 = 0.7$, $w_2 = 0.2$ and $w_3 = 0.1$. The UD values were found for each SSA and the results are given in Tables 4 and 5. As can be seen from Table 4, if the weight coefficient decreases in the fitness function of the cost, the cost increases, while the cost decreases in the opposite case. However, in Table 5, if the weight coefficient of the UD is increased by a factor of two, the total waiting time reduces from 13 h to 7 h compared to the best starting time. If the weight coefficient of the PAR is doubled, the total waiting time decreases from 13 h to 10 h.

Table 4. Comparison of the cost for various HEMS1.

SHA	HEMS1a	HEMS1b	HEMS1c
TO	9.8	19.6	19.6
IR	10.1	13.4	13.4
VC	11.6	11.6	11.6
MW	14.9	14.9	14.9
KE	9.2	12.2	9.2
AC	117.1	127.7	117.1
WM	30.2	44.7	33.7
CD	16.2	29.7	29.7
CO	10.5	10.5	10.9
DW	22.7	22.7	22.7
SH	20.5	20.5	20
HD	8.0	8.0	8.1

Table 5. Comparison of the UD for various HEMS1.

SHA	HEMS1a	HEMS1b	HEMS1c
TO	−1	0	0
IR	−1	0	0
VC	1	1	1
MW	0	0	1
KE	−1	0	−1
AC	5	4	5
WM	4	0	1
CD	4	0	1
CO	1	1	0
DW	1	1	0
SH	0	0	1
HD	0	0	1

Second, with the same weight coefficient sets, the optimal cost and the UD in various HEMS2 were found for each SSA and the results are given in Tables 6 and 7. Similarly, Table 6 shows that if the weight coefficient in the fitness function of the cost is large, the cost decreases, and on the contrary, the cost is larger. In addition, when the weight coefficient of the UD increases by a factor of two, it can be seen from Table 7 that the number of SSAs starting to work at the best hour increases and the total waiting time decreases to 10 h. If the weight coefficient of the PAR is doubled, the total waiting time increases to 16 h. That is, the waiting time, which is 10 h in the first case under the same conditions, increases by 60% in the second case to 16 h. The average cost in the three operation cases of HEMS1 and HEMS2 is 25.8¢ and 27.2¢, respectively. Specifically, there is a 1.4¢ increase in the

DC of SSAs. Overall, the average cost decreases from 645.1¢ to 423.8¢ in the HEMS1 and HEMS2 operation conditions, respectively, the average UD increases from 7.7 to 8.7 h and the average PAR decreases from 2.73 to 2.32. In terms of the loads and operation conditions, the average cost in HEMS2 is 34.3% less than in HEMS1, the average UD in HEMS2 is 1 h more than in HEMS1 and the average PAR in HEMS1 is 15.1% less than in HEMS2. In this example application, it is seen that the PV system and ESS reduce the DC by 34.3%. When projecting over 20 years, the levelized cost of energy (LCOE) for the current system is found to be around 4.9¢/kWh. Here, the LCOE is calculated as the ratio of USD4519.70, which is the investment and maintenance/repair cost reflected over 20 years, to 91,980 kWh, which is the average amount of energy produced by the system over 20 years.

Table 6. Comparison of the DC for various HEMS2.

SHA	HEMS2a	HEMS2b	HEMS2c
TO	19.6	19.6	21.6
IR	13.4	13.4	10.1
VC	19.3	18.9	19.3
MW	15.5	14.9	15.5
KE	12.2	9.2	9.2
AC	117.1	127.7	117.1
WM	33.0	44.7	33
CD	29.2	29.7	29.2
CO	10.9	10.9	10.9
DW	22.7	22.7	22.7
ES	20.0	20.0	20
HD	8.1	8.1	8.1

Table 7. Comparison of the UD for various HEMS2.

SHA	HEMS2a	HEMS2b	HEMS2c
TO	0	0	1
IR	0	0	−1
VC	−1	−2	−1
MW	−1	1	−1
KE	0	−1	−1
AC	5	4	5
WM	2	0	2
CD	2	0	2
CO	0	0	0
DW	0	0	0
ES	1	1	1
HD	1	1	1

Looking more closely into the cost contribution of the PV system and ESS in HEMS2, it can be seen from Figures 9 and 10 that the power needed for the load is supplied from the PV system and ESS when the EP is high and from the grid when it is low. As can simply be seen from Figures 9 and 10, in all three sets of weight coefficients, the demanded power is mostly met from the PV system and the ESS in the time intervals when the EP is high, thus reducing the cost. When the change in the three weight coefficient sets is examined, it is seen that the power demanded from the grid is larger between slots 9 and 13 when the weight coefficient of the UD is large. The power transferred from the ESS to the load in all three weight coefficient sets was between slots 8 and 14. As expected, the maximum power transferred in a slot was 0.95 kW. From the above results, it is seen that the weight coefficients are considerably influential on the objective function values.
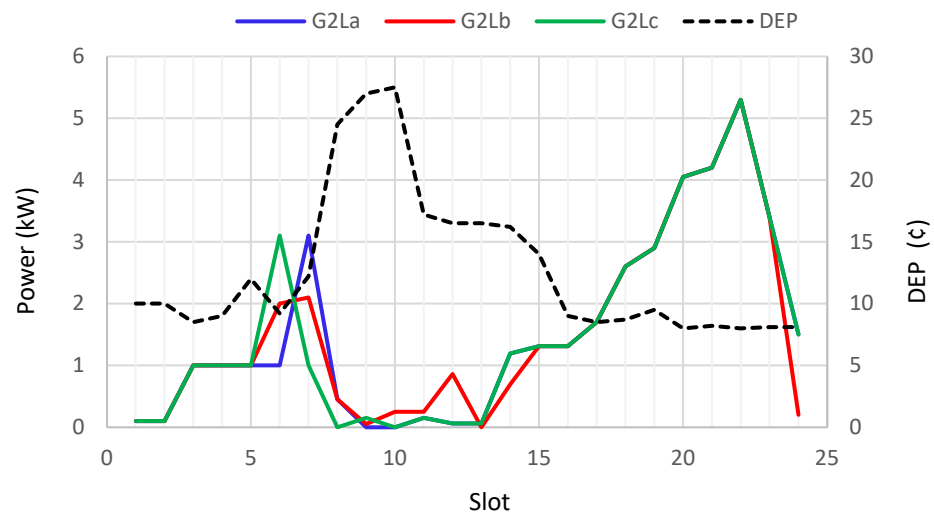
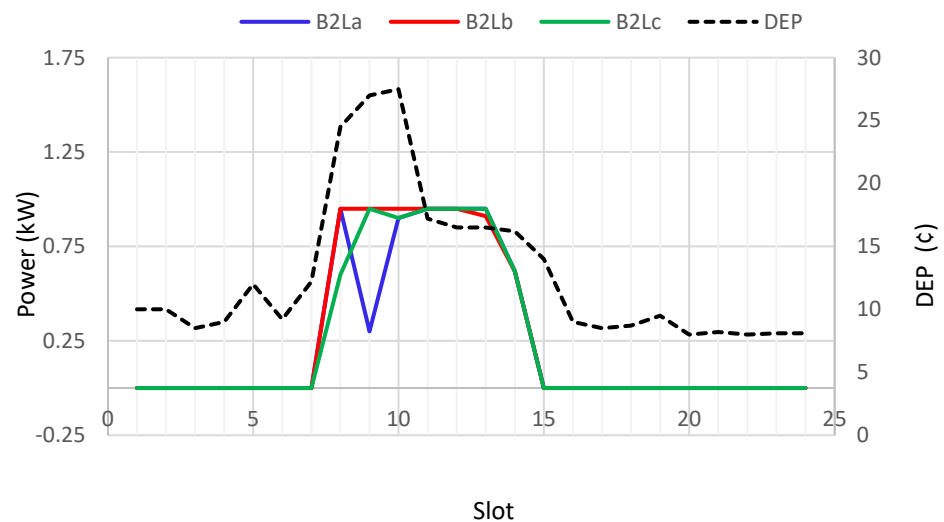**Figure 9.** Power absorbed from the grid for various weight numbers.

Figure 10. Power discharge from the ESS for various weight numbers.

In order to fully understand this effect on the DC, the PAR and the UD values were found for HEMS1 and HEMS2 by maintaining the PAR's weighting coefficient constant at 0.1 under current conditions, and the results are given in Tables 8 and 9. As can be seen from Tables 8 and 9, it is seen that in HEMS1 and HEMS2, as the weight coefficient of the cost decreases, the total cost increases; on the other hand, as the weighting coefficient of the UD increases, the total UD decreases as expected. Although this is an expected case, the effects of the weight coefficients were determined quantitatively in this study.

Table 8. Effects of the weight numbers on the objectives in the HEMS1.

Case	w_1	w_2	w_3	Cost (¢)	PAR	UD
I	0.8	0.1	0.1	616.8	2.94	10
II	0.7	0.1	0.2	671.5	2.94	6
III	0.6	0.1	0.3	690.6	2.93	5
IV	0.5	0.1	0.4	708.8	2.58	4
V	0.4	0.1	0.5	725.6	2.37	3

Table 9. Effects of weight numbers on the objectives in the HEMS2.

Case	w_1	w_2	w_3	Cost (¢)	PAR	UD
I	0.8	0.1	0.1	616.8	2.94	10
II	0.7	0.1	0.2	671.5	2.94	6
III	0.6	0.1	0.3	690.6	2.93	5
IV	0.5	0.1	0.4	708.8	2.58	4
V	0.4	0.1	0.5	725.6	2.37	3

In Table 10, B2L and G2B powers were compared with a previous study [8]. According to Table 10, while G2B was 7 kWh in the proposed study, it was 7.05 kWh in [8]. While B2L was 1.51 kWh in [8], the B2La, B2Lb and B2Lc values were found to be 5.62, 6.28 and 5.92 kWh, respectively, in the present study. The reason for this obvious difference is that in the previous study [8], the energy produced from PV was first stored in the ESS and the surplus energy was transferred to the grid.

Table 10. Comparison of G2B and B2L with those obtained from previous work [8].

Slot	G2B [8]	G2B	B2L [8]	B2La	B2Lb	B2Lc
1	1	1	0	0	0	0
2	1	1	0	0	0	0
3	1	1	0	0	0	0
4	1	1	0	0	0	0
5	1	1	0	0	0	0
6	1	1	0	0	0	0
7	1	1	0	0	0	0
8	0	0	0.43	0.95	0.95	0.6
9	0	0	0	0.3	0.95	0.95
10	0	0	0	0.9	0.95	0.9
11	0	0	0	0.95	0.95	0.95
12	0	0	0.06	0.95	0.95	0.95
13	0	0	0.06	0.95	0.91	0.95
14	0	0	0.06	0.618	0.618	0.618
15	0	0	0	0	0	0
16	0	0	0	0	0	0
17	0.05	0	0	0	0	0
18	0	0	0	0	0	0
19	0	0	0.903	0	0	0
20	0	0	0	0	0	0
21	0	0	0	0	0	0
22	0	0	0	0	0	0
23	0	0	0	0	0	0
24	0	0	0	0	0	0

In the present study, the energy stored from the ESS directly feeds the load, and the surplus is delivered to the grid. In the previous study, there is a disadvantageous case that affects the total system efficiency, since the energy sales to the grid are realized only through the ESS, but as explained earlier, this disadvantage is not the case in this study. It is certain that the results given in the graphs and tables above will increase if the installed capacity of the PV system or the charge and discharge rates of the ESS in one slot are increased.

For example, a 1.5-times increase in the maximum power produced by the PV system or 2 kW of power transferred to or from the ESS in an hourly time period is certain to have a significant impact on the daily energy cost.

In order to compare the results with the previous study, the maximum power produced by the PV system was increased by 1.5 times and Table 10 was rearranged. The results are given in Table 11.

Table 11. Comparison of G2B and B2L with those obtained from previous work [8]. The PV power was in-creased with respect to the results shown in Table 10, as explained in the text.

Slot	G2B [8]	G2B	B2L [8]	B2La	B2Lb	B2Lc
1	1	1	0	0	0	0
2	1	1	0	0	0	0
3	1	1	0	0	0	0
4	1	1	0	0	0	0
5	1	1	0	0	0	0
6	1	1	0	0	0	0
7	1	1	0	0	0	0
8	0	0	0.43	0.95	0.95	0.95
9	0	0	0	0	0	0
10	0	0	0	0	0	0
11	0	0	0	0.95	0	0.95
12	0	0	0.06	0	0.95	0.95
13	0	0	0.06	0	0	0.95
14	0	0	0	0	0.415	0.618
15	0	0	0	0	0	0
16	0	0	0	0	0	0
17	0.339	0	0	0	0	0
18	0	0	0	0	0	0
19	0	0	0.903	0	0	0
20	0	0	0	0	0	0
21	0	0	0	0	0	0
22	0	0	0	0	0	0
23	0	0	0	0	0	0
24	0	0	0	0	0	0

According to Table 11, while the G2B was 7.34 kW in total in the previous study, it is 7 kWh in this study. In addition, while B2L was 1.45 kWh in the previous study, it was found to be 1.90, 2.32 and 4.42 kWh in this study, depending on the weight coefficients. When the coefficient of UD is 0.2, there is more power transfer from the ESS to the load. It can be said that the SSAs operating close to the best starting times are influential on this. Table 12 gives the PV2G and B2G power variations with the slot and as can be seen from Table 12, the PV2Ga is larger than PV2Gb and PV2Gc. This implies that more energy sales to the grid are required for a lower cost in the whole system. When HEMS2 and HEMS3 are compared in terms of energy sales to the grid, it is seen that while there are no sales in the first, there are sales in the second. From one perspective, this is related to the change in the installed power of the EP, the PV system and the amount of SR during the day.

It is apparent that increasing the PV capacity by 50% will naturally lead to a change in the G2L values at different values of weight coefficients. In Figure 11, it can be seen that the G2L is quite small, as expected between 8:00 and 18:00, when the PV produces intense power. At other times, it reaches 3.1 kW in the morning and 6.7 kW in the afternoon. The G2L change in HEMS2 remains the same in the morning and the G2L change in HEMS3 decreases to 5.3 kW in the afternoon. In general, the change trends in both HEMS are similar, as the EP change seems to be quite effective here. On the other hand, looking into the B2L changes in Figure 12, it is seen that HEMS2 and HEMS3 show a similar trend and the power transferred from the ESS to the load is higher in the time periods when the EP is high. Although PV2G in HEMS2 is zero in all time periods, as seen in Figure 13, PV2G in HEMS3 varies between 0.3 and 0.585 kW between 10.00 and 14.00 h.

In other words, where the current load and DEP are concerned, it is certain that the PV2G values will play a significant role in reducing the total DC as the capacity of the PV system increases.

When a general evaluation of the results given above is made, the single-objective cost-minimization problem of an HEMS with dynamic EP, ESS and PV can be solved simply in a deterministic way with the available data, and thus, the lowest DC can be found.
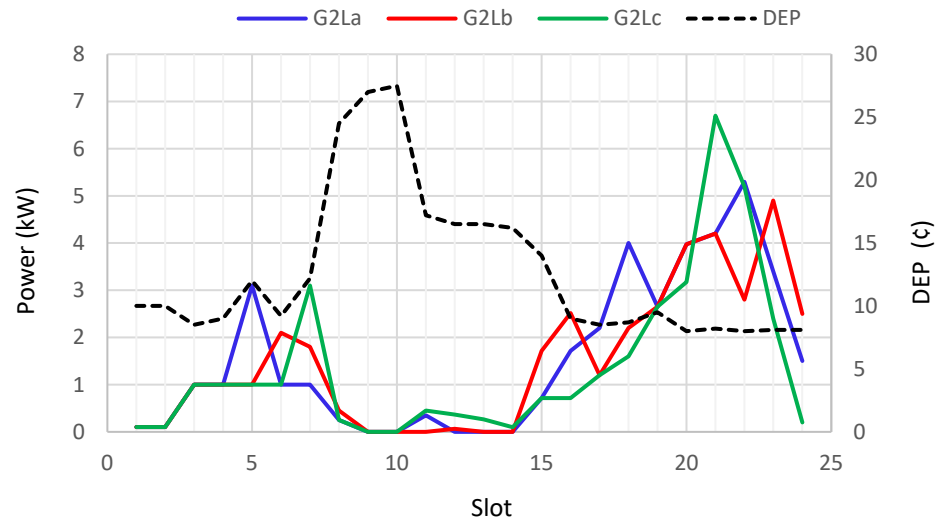
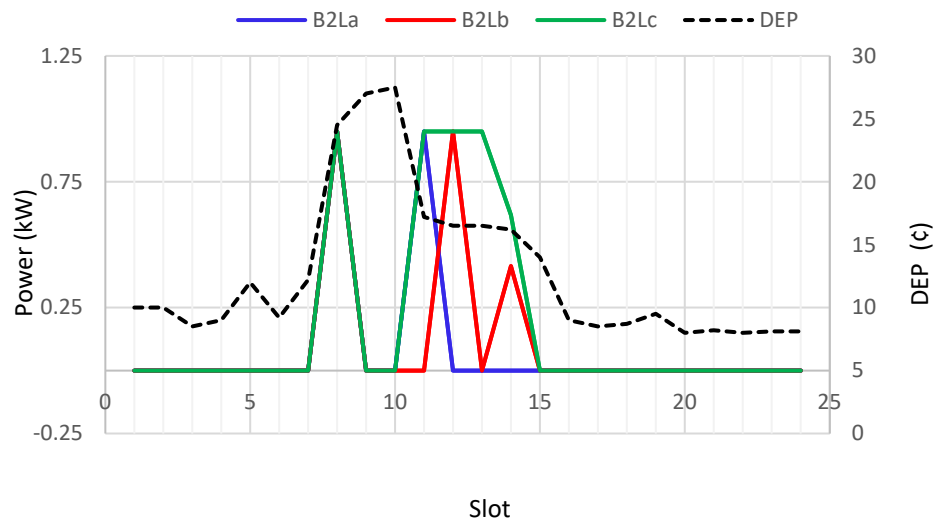**Figure 11.** Power absorbed from the grid with increasing PV capacity.

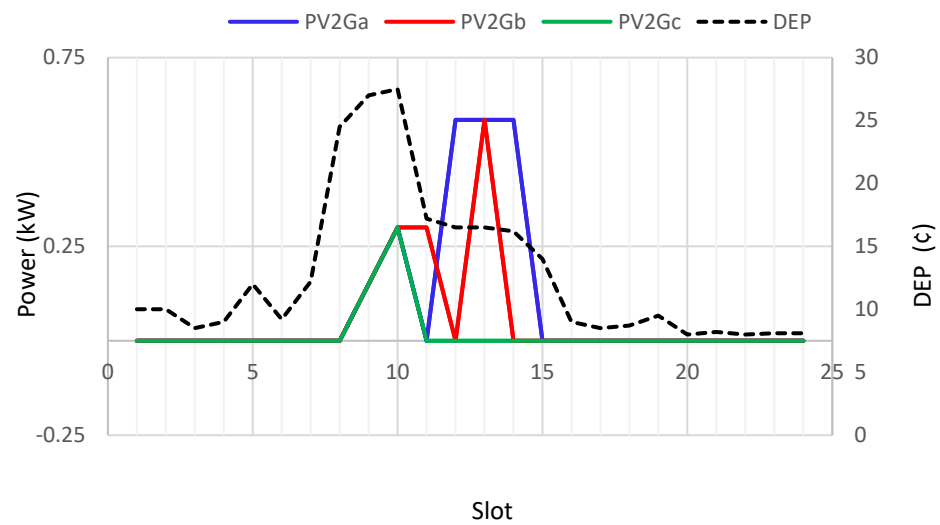**Figure 12.** Power discharge from the ESS with increasing PV capacity.

Figure 13. Power delivery with increasing PV capacity.

Table 12. Comparison of PV2G and B2G with previous work [8].

Slot	PV2B [8]	B2G [8]	PV2Ga	PV2Gb	PV2Gc
1	0	0	0	0	0
2	0	0	0	0	0
3	0	0	0	0	0
4	0	0	0	0	0
5	0	0	0	0	0
6	0	0	0	0	0
7	0	0	0	0	0
8	0	0.57	0	0	0
9	0	1	0.15	0.15	0.15
10	0	1	0.3	0.3	0.3
11	0	1	0	0.3	0
12	0	0.94	0.585	0	0
13	0	0.94	0.585	0.585	0
14	0.51	0	0.585	0	0
15	0	0.78	0	0	0
16	0	0	0	0	0
17	0.661	0	0	0	0
18	0	0	0	0	0
19	0	0	0	0	0
20	0	0	0	0	0
21	0	0	0	0	0
22	0	0	0	0	0
23	0	0	0	0	0
24	0	0	0	0	0

In addition to the cost, considering two other objectives such as the PAR and the UD, the multi-objective minimization problem can be solved with the SFLA technique depending on the available data and appropriate weight coefficients; hence, the lowest DC, PAR and UD can be computed.

The current results are based on a single EP and PV dataset and of course, the obtained results inevitably change as the EP and PV datasets change. However, it is more reasonable to use a single EP and PV dataset in order to examine the results obtained without confusion. In addition, with a single EP and PV dataset, it is possible to more clearly see the effects of the weighting coefficients on the results in the multi-objective optimization process. As the weight coefficient increases, the value of the objective function is expected to be smaller and smaller, and this is tabulated for each HEMS. Another point is that the UD value of each SSA can be calculated according to the early or late start time according to the best start time and normalized during the optimization process to find the optimal UD value.

Here, only one of the early or late operation times falling in the same time period is taken as the late or early operation time. This provides a significant savings in total the DC in dynamic EP cases involving PV and ESS. In an HEMS's 20-year life-time projection, the PV and ESS remain less than 10% of the total revenue in terms of installation and maintenance costs. As a result, it is always possible to use an HEMS with PV and ESS more efficiently with optimal scheduling for dynamic EP. The results obtained from the dataset used in this study have provided a better understanding of the importance of the HEMS for future work.

4. Conclusions

In this study, we designed and assessed three types of HEMS, namely HEMS1, HEMS2 and HEMS3. HEMS1 is composed of a metering infrastructure, a smart energy meter, a home gateway and an EMC. HEMS2 is formed by adding a 1.8 kWp PV system and a 10 kWh ESS to HEMS1. HEMS3 is obtained by increasing the PV-system power in HEMS2 by 50%. The HEMS2 is designed to demonstrate the impact of PV and ESS on the DC, the

PAR and the UD objectives. HEMS3 is designed to show the effect on existing objectives in the case of increasing PV system power.

All three HEMS require solving a single-objective and a tri-objective minimization problem. Such problems have been or are currently being solved using a limited number of metaheuristics under different conditions using some datasets. In the proposed method, the operation and non-operational status of each electrical household appliance in a 24 h period is represented by a 24-bit binary number. Adhering to the defined constraints, the global optimum starting times to minimize the available objectives were found using the SFLA and the binary-coded crossover and mutation GA operators. For better results, a binary-coded crossover algorithm was developed specific to the problem.

Comparing the simulation results with those obtained from HEMS1 and HEMS2 shows that there are 32.2% and 44.4% improvements in cost respectively, respectively. As can be seen from Figure 8, it is observed that the PV system and ESS in single-objective optimization are quite effective in reducing the daily consumption cost under the current conditions. It is apparent that this is due to the fact that the PV system produces the most power during the most expensive noon hours, when energy is most needed. In this respect, the importance of integrating the PV system into homes as an additional power source becomes evident here once again. Furthermore, the effect of the ESS should not be ignored. Although the combination of these two systems is initially high in terms of maintenance and investment costs, it presents an advantageous situation for a total system life of 20–25 years. It should be emphasized here that when projecting the savings of one day on 20 years, the DC of installation and maintenance of PV and ESS is around 5¢, while the contribution of PV and ESS to the DC is around 221¢.

A comparison of Tables 3 and 4 shows that the cost of each electrical HA increases in the case of multi-objective optimization. In fact, this is to be expected, as reducing the PAR and UD objectives will inevitably increase the daily consumption cost. This increase in cost varies depending on the values of the selected weight coefficients. In other words, the objectives with an increased weight coefficient receive lower values; otherwise, it takes larger values. For example, as given in Table 5, as the coefficient of the UD objectives increases, it is seen that the electrical appliances approach the best working hours. In addition, it should be noted here that the power delivered from the grid or ESS to the load differ in case the coefficients change based on the graph given in Figures 9 and 10; thus, it is possible to see the effect of the weight coefficient very clearly from Tables 8 and 9.

In multi-objective optimization, it is seen that when the installed PV power increases, the cost from the grid decreases, so the power purchased from the grid decreases considerably, especially at noon. On the other hand, it is observed that the power transferred from the ESS to the load and from the PV system to the grid increases.

Nomenclature

AC	Air conditioner
AI	Artificial intelligence
ANN	Artificial neural network
B2L	Power flow from ESS to load
BA	Bat algorithms
BFO	Bacterial foraging optimization
BSS	Best start slot
CD	Cloth dryer
CO	Electric cooker
DC	Daily energy consumption cost
DE-CSFLA	Differential evolution-chaos SFLA
DEP	Dynamic electricity pricing
DRLA	Deep reinforcement learning algorithm
DW	Dish washer
EMC	Energy management controller
ES	End slot
ESS	Energy-storage system
EV	Electric vehicle
G2B	Power flow from grid to ESS
G2L	Power flow from grid to load
GA	Genetic algorithms
GWO	Grey wolf optimization
HA	Home appliance
HD	Hair dryer
HEMS	Home energy management
HEMS1a	MOO in HEMS1 for a set of $w_1 = 0.8$, $w_2 = 0.1$ and $w_3 = 0.1$
HEMS1b	MOO in HEMS1 for a set of $w_1 = 0.7$, $w_2 = 0.1$ and $w_3 = 0.2$
HEMS1c	MOO in HEMS1 for a set of $w_1 = 0.7$, $w_2 = 0.2$ and $w_3 = 0.1$
HEMS2a	MOO in HEMS2 for a set of $w_1 = 0.8$, $w_2 = 0.1$ and $w_3 = 0.1$
HEMS2b	MOO in HEMS2 for a set of $w_1 = 0.7$, $w_2 = 0.1$ and $w_3 = 0.2$
HEMS2c	MOO in HEMS2 for a set of $w_1 = 0.7$, $w_2 = 0.2$ and $w_3 = 0.1$
IR	Iron
IPM	Interior Point Method
KE	Kettle
L	Time length
LCSS	Least cost start slot
LI	Lighting
LP	Linear programming
MILP	Mixed-integer linear programming
ML	Machine learning
MOO	Multi-objective optimization
MPPT	Maximum power point tracker
MW	Microwave
NSHA	Non-shiftable HA
OCDM	Optimal condition decomposition method
P	Average power
PAR	Peak-to-average ratio
PC	Personal computer
PSO	Particle swarm optimization
PV	Photovoltaic
PV2G	Power flow from PV to grid
PV2L	Power flow from PV to load
RES	Renewable energy sources
RG	Refrigerator
SC	Security cameras
SFLA	Shuffled frog-leaping algorithm

SH	Electric shower
SHA	Shiftable HA
SR	Solar radiation
SS	Start slot
TO	Toaster
TV	Television
UD	User's discomfort
VC	Vacuum cleaner
WDC	Weather data center
WDO	Wind-driven optimization
WM	Washing machine

References

1. Bouakkaz, A.; Gil Mena, A.J.; Haddad, S.; Ferrari, M.L. Efficient energy scheduling considering cost reduction and energy saving in hybrid energy system with energy storage. *J. Energy Storage* **2021**, *33*, 101887. [CrossRef]
2. Mohammad, A.; Zuhaib, M.; Ashraf, I. An optimal home energy management system with integration of renewable energy and energy storage with home to grid capability. *Int. J. Energy Res.* **2022**, *46*, 8352–8366. [CrossRef]
3. Ahmad, A.; Khan, A.; Javaid, N.; Hussain, H.M.; Abdul, W.; Almogren, A.; Niaz, I.A. An Optimized Home Energy Management System with Integrated Renewable Energy and Storage Resources. *Energies* **2017**, *10*, 549. [CrossRef]
4. Dinh, H.T.; Yun, J.; Kim, D.M.; Lee, K.-H.; Kim, D. A Home Energy Management System with Renewable Energy and Energy Storage Utilizing Main Grid and Electricity Selling. *IEEE Access* **2020**, *8*, 49436–49450. [CrossRef]
5. Merdanoğlu, H.; Yakıcı, E.; Doğan, O.T.; Duran, S.; Karatas, M. Finding optimal schedules in a home energy management system. *Electr. Power Syst. Res.* **2020**, *182*, 106229. [CrossRef]
6. Wang, X.; Mao, X.; Khodaei, H. A multi-objective home energy management system based on internet of things and optimization algorithms. *J. Build. Eng.* **2020**, *33*, 101603. [CrossRef]
7. Amer, A.; Shaban, K.; Gaouda, A.; Massoud, A. Home Energy Management System Embedded with a Multi-Objective Demand Response Optimization Model to Benefit Customers and Operators. *Energies* **2021**, *14*, 257. [CrossRef]
8. Dinh, H.T.; Lee, K.; Kim, D. Supervised-learning-based hour-ahead demand response for a behavior-based home energy management system approximating MILP optimization. *Appl. Energy* **2022**, *321*, 119382. [CrossRef]
9. Ma, Y.; Chen, X.; Wang, L.; Yang, J. Study on Smart Home Energy Management System Based on Artificial Intelligence. *J. Sens.* **2021**, *2021*, 9101453. [CrossRef]
10. Song, Z.; Guan, X.; Cheng, M. Multi-objective optimization strategy for home energy management system including PV and battery energy storage. *Energy Rep.* **2022**, *8*, 5396–5411. [CrossRef]
11. Koltsaklis, N.; Panapakidis, I.; Christoforidis, G.; Knápek, J. Smart home energy management processes support through machine learning algorithms. *Energy Rep.* **2022**, *8*, 1–6. [CrossRef]
12. Chakir, A.; Abid, M.; Tabaa, M.; Hachimi, H. Demand-side management strategy in a smart home using electric vehicle and hybrid renewable energy system. *Energy Rep.* **2022**, *8*, 383–393. [CrossRef]
13. Lissa, P.; Deane, C.; Schukat, M.; Seri, F.; Keane, M.; Barrett, E. Deep reinforcement learning for home energy management system control. *Energy AI* **2021**, *3*, 100043. [CrossRef]
14. Huang, J.; Koroteev, D.D.; Rynkovskaya, M. Machine learning-based demand response in PV-based smart home considering energy management in digital twin. *Sol. Energy* **2023**, *252*, 8–19. [CrossRef]
15. Parandeh, K.; Bagheri, A.; Jadid, S. Optimal Day-ahead Dynamic Pricing of Grid-connected Residential Renewable Energy Resources Under Different Metering Mechanisms. *J. Mod. Power Syst. Clean Energy* **2023**, *11*, 168–178. [CrossRef]
16. Debataa, S.; Kumar, S.C.; Panigrah, S.P. Efficient energy management strategies for hybrid electric vehicles using shuffled frog-leaping algorithm. *Int. J. Sustain. Eng.* **2015**, *8*, 138–144. [CrossRef]
17. Fang, G.; Guo, Y.; Wen, X.; Fu, X.; Lei, X.; Tian, Y.; Wang, T. Machine learning-based demand response in PV-based smart home considering energy management in digital twin. *Water Resour. Manag.* **2018**, *32*, 3835–3852. [CrossRef]